

First-order asymptotics for the eigenfrequencies of the Earth and application to the retrieval of large-scale lateral variations of structure

Barbara Romanowicz and Geneviève Roult *Laboratoire de Sismologie, Institut de Physique du Globe, 4 Place Jussieu, Tour 14, F-75230 Paris cedex 05, France*

Accepted 1986 March 24. Received 1986 March 19; in original form 1985 August 19

Summary. We present a variety of examples, showing systematic fluctuations as a function of angular order of measured eigenfrequencies for given normal modes of the Earth. The data are single station measurements from the GEOSCOPE network. Such fluctuations are attributed to departures from the lowest order asymptotic expression of the geometrical optics approximation. We derive first-order asymptotic expressions for the location parameter for all three components of the Earth's motion, by a method based on the stationary phase approximation and geometric relations on the unit sphere.

We illustrate the sensitivity of the fluctuations to the different parameters involved (source parameters, epicentral distance, laterally heterogeneous earth model) with synthetic examples corresponding to GEOSCOPE observations. Finally, we show the results of first attempts at inversion, which indicate that, when the fluctuations are taken into account, more accurate estimates of the great circle average eigenfrequencies can be obtained, and additional constraints put on the structure in the neighbourhood of the great circle.

Key words: normal modes, asymptotics

1 Introduction

When interpreting measurements of the frequencies of free oscillations of the Earth, it is generally assumed that the geometrical optics approximation is valid in its lowest order expression. This implies that the centre frequency $\Omega_K(l)$ of mode K , corresponding to large angular orders l , is related to the average, over the great circle γ containing the source and the station, of the local frequency $\delta\omega_0$ (Jordan 1978; Dahlen 1979):

$$\Lambda_K = \Omega_K(l) - \Omega_{\text{ref}}(l) = \frac{1}{2\pi} \int_{\gamma} \delta\omega_0(s) ds, \quad (1)$$

where Ω_{ref} is the corresponding eigenfrequency calculated for a reference spherically-

symmetric model. Following Jordan (1978), Λ_K is also called the 'location parameter'. Λ_K thus depends only on the average structure underlying the great circle path and is independent of the relative location on γ of the source and receiver, of the structure outside γ and of the parameters of the seismic source. In particular, the predicted variations of eigenfrequency with angular order l are smooth.

In what follows, we shall define the apparent centre frequency Ω of mode K as the peak frequency of the power spectrum corresponding to a given angular order l . Although much debate has been devoted to defining the centre frequency correctly, Silver & Jordan (1981) have shown that, for frequencies higher than 1 mHz, all the definitions are equivalent.

In practice it is often observed that, for a given mode-branch, the variations of measured eigenfrequencies with angular order are very rugged and the fluctuations appear to have some sort of periodicity.

This has been systematically observed on very long period data from stations run by IPG in Paris (Jobert & Roullet 1976) and has led these authors to design a smoothing procedure to eliminate such fluctuations in the measurement of great circle phase velocities based on free oscillation data. More recently, such observations have also been made on data from the GEOSCOPE network (Roullet & Romanowicz 1984; Roullet, Romanowicz & Jobert 1986).

Systematic fluctuations of order 2 were also reported by Silver & Jordan (1981) for three

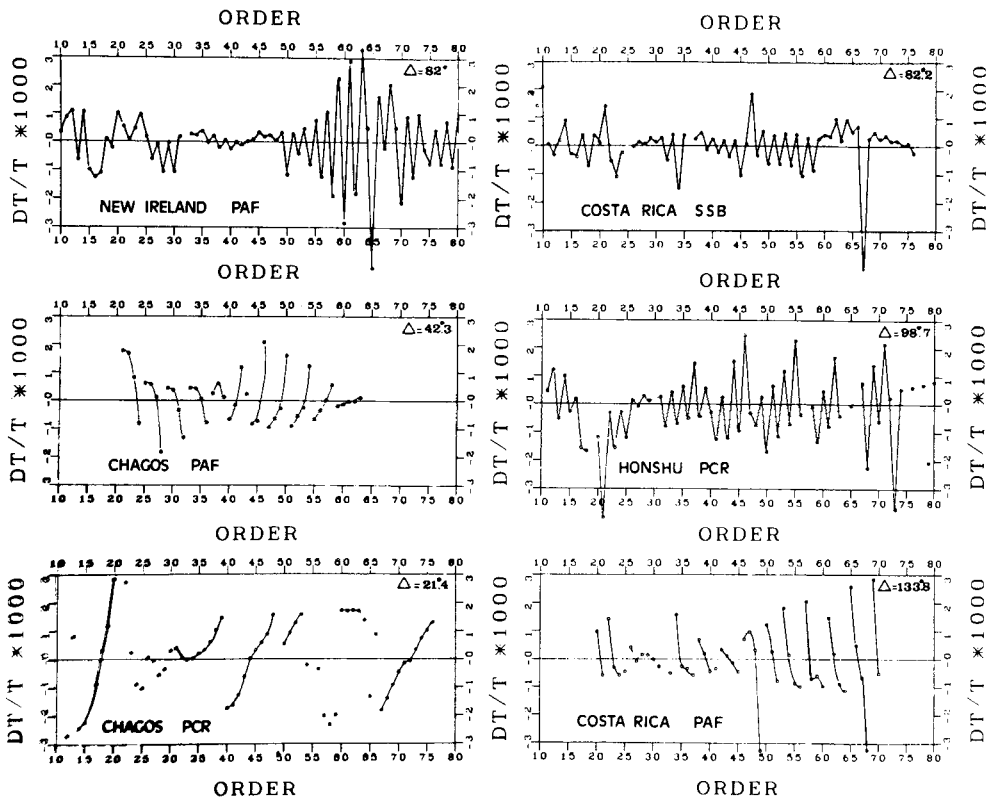


Figure 1. Examples of fundamental mode eigenfrequency measurements on vertical records from the GEOSCOPE network, showing systematic fluctuations as a function of angular order, with periodicity depending on the epicentral distance. The data are expressed as relative differences with respect to the PREM model and variable filtering has been applied to the records to isolate the fundamental spheroidal mode. The smooth part of the observations has been removed by high pass filtering.

Kermadec events of 1976 with similar focal mechanisms. These authors pointed out that such effects could contribute significantly to the large unexplained part of the variance in global eigenfrequency data, and first suggested that they could be due to departures from the geometrical optics approximation as commonly applied. In order to explain these observations, Dahlen (1982, unpublished) proposed a first-order asymptotic expression for the location parameter, in the case of an isotropic source, which led him to introduce a term in $(1/l)$ proportional to

$$\tan \left(k\Delta - \frac{\pi}{4} \right),$$

where Δ is the epicentral distance and $k = l + 1/2$. The derivation of this expression, in the case of an isotropic source, has since been reported in Davis & Henson (1986).

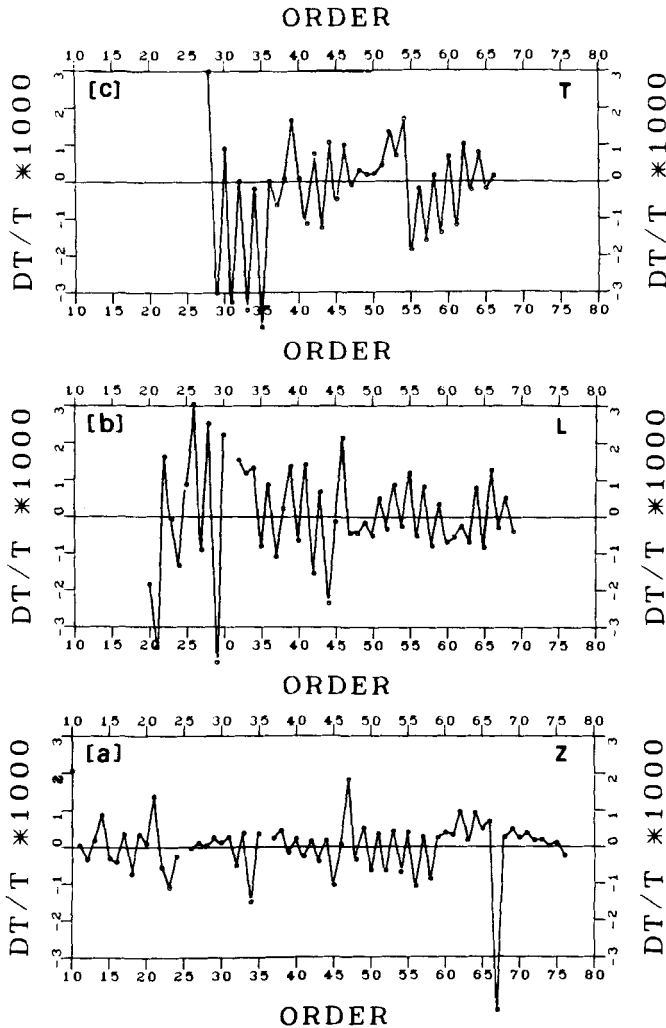


Figure 2. Example of order 2 fluctuations of measured eigenfrequencies as a function of angular order for the fundamental mode, extracted by variable filtering from the three component records of the Costa Rica event of 1983 April 3, observed at GEOSCOPE station SSB ($\Delta = 82.45^\circ$). (a) vertical; (b) longitudinal; (c) transverse. The notations are as in Fig. 1.

Most reported observations of such fluctuations have, so far, been on vertical records and for distances close to 90° , for which the periodicity in l is 2, and for the fundamental mode. The greater variety of observations now available from the GEOSCOPE network (Romanowicz *et al.* 1984) strongly confirm Dahlen's conjecture. As shown in a series of examples on Fig. 1, they are clearly observed for different epicentral distances, with the periodicity as predicted by Dahlen's

$$\tan \left(k\Delta - \frac{\pi}{4} \right)$$

term (4 for Δ close to 45° or 135° , 8 for Δ close to $21^\circ \dots$). Epicentral data for the events considered can be found in Roullet *et al.* (1986). We also see the fluctuations on all three components: Fig. 2 gives such an example for the Costa Rica event of 1983 April 3, observed at the GEOSCOPE station SSB in France. In some cases, after variable filtering has been applied to isolate a given mode (Roullet & Romanowicz 1984), they are also visible on overtone spectra. Fig. 3 gives an example for the same event observed on the vertical component at SSB. Here, the second spheroidal overtone has been extracted and order two fluctuations are clearly visible.

It thus appears that some systematic account of these observations needs to be taken, and

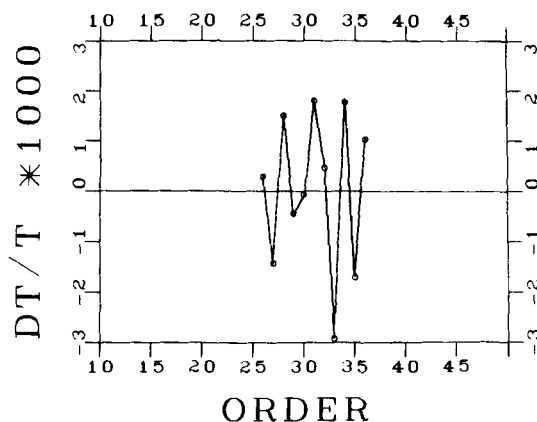


Figure 3. Example of order 2 fluctuations observed on eigenfrequencies corresponding to the second spheroidal overtone, extracted by variable filtering from the vertical component record of the Costa Rica event of 1983 April 3, observed at SSB ($\Delta = 82.45^\circ$). The notations are as in Fig. 1.

higher order asymptotics is a promising approach. In what follows, we first present an alternative derivation of the first-order asymptotic expressions for the location parameter, for each of the three components of the ground motion and for the case of a general moment tensor source. Our independent derivation differs from that of Dahlen in that it is based on geometrical relations on the sphere and on the physically tangible stationary phase approximation.

In the second part of this paper, we present the results of experiments designed to test the sensitivity of the observed eigenfrequency, as a function of angular order l , to the different parameters involved: source mechanism and depth, epicentral distance and earth model. We show how the introduction of first-order asymptotics can be used to improve the quality of the measurement and interpretation of great circle averages, and to put better constraints on the large-scale global models of the Earth's structure.

2 First-order asymptotics for the location parameter

Following Jordan (1978) and Dahlen (1979), the location parameter Λ_K can be expressed as:

$$\Lambda_K = \frac{\sum_{mm'} S_m^K(\theta_s, \phi_s) H_{mm'}^K \cdot R_m^K \cdot (\theta_r, \phi_r)}{\sum_m S_m^K(\theta_s, \phi_s) R_m^K(\theta_r, \phi_r)} \quad (2)$$

where $\{H_{mm'}^K\}$ is the splitting matrix corresponding to mode K (Woodhouse & Dahlen 1978), (θ_s, ϕ_s) and (θ_r, ϕ_r) are respectively the coordinates of the epicentre and of the receiver. S_m^K and R_m^K are source and receiver functions respectively, and can be written in condensed form, using an operator formalism

$$R_m^K(\theta_r, \phi_r) = \mathbf{v} \cdot \mathbf{D} Y_l^m(\theta_r, \phi_r)$$

where \mathbf{D} is the displacement operator, \mathbf{v} the instrument operator (instrument response and component), and Y_l^m are fully normalized spherical harmonics (Edmonds 1960). Also:

$$S_m^K(\theta_s, \phi_s) = \mathbf{M} : \epsilon^* Y_l^m(\theta_s, \phi_s) = \mathbf{M} : \epsilon Y_l^{m*}(\theta_s, \phi_s)$$

where \mathbf{M} is the moment tensor describing the source and ϵ is the strain operator.

Woodhouse & Girnius (1982) have shown that expression (2) can be written in terms of three local functionals $\delta\omega_i$ ($i = 1, 3$) of the Earth's structure:

$$\Lambda_K = \sum_{i=0}^2 \iint \delta\omega_i^K(\theta, \phi) K_i(\theta, \phi) ds \quad (3)$$

with:

$$\delta\omega_i^K = [2l(l+1)]^i \int_0^a \delta\mathbf{m}(r, \theta, \phi) \{M_K^{(i)}(r) r^2 dr - \Sigma \mathbf{h}(\theta, \phi) [H_K^{(i)}]^\pm\}.$$

Here $\delta\mathbf{m}$ and \mathbf{h} represent the perturbations to a reference spherical earth model and $M_K^{(i)}$, $H_K^{(i)}$ are given in Woodhouse & Girnius (1982) in terms of eigenfunctions of the reference model. In expression (3), the surface integral is taken over the unit sphere and the kernels K_i are:

$$K_i(\theta, \phi) = \frac{\sum_{mm'} S_m^K(\theta_s, \phi_s) (-\nabla_1^2)^i [Y_l^m(\theta, \phi) Y_l^{m'}(\theta, \phi)] R_m^K(\theta_r, \phi_r)}{[2l(l+1)]^i \sum_m S_m^K(\theta_s, \phi_s) R_m^K(\theta_r, \phi_r)} \quad (4)$$

where ∇_1 is the gradient operator on the unit sphere. We note here that $\delta\omega_0$ is the local frequency as defined in Jordan (1978). Using the operator formalism introduced above, since the operators do not depend on m and m' , the kernels K_i become:

$$K_i(\theta, \phi) = \frac{\text{Op}_N^i \left[\sum_{mm'} Y_l^{m*}(\theta_s, \phi_s) Y_l^m(\theta, \phi) Y_l^{m'}(\theta, \phi) Y_l^{m'}(\theta_r, \phi_r) \right]}{[2l(l+1)]^i \text{Op}_D [\Sigma Y_l^{m*}(\theta_s, \phi_s) Y_l^m(\theta_r, \phi_r)]} \quad (5)$$

where we have defined the two operators:

$$\begin{aligned}\text{Op}_N^i &= (\mathbf{M} : \epsilon) (-\nabla_1^2)^i (\mathbf{v} \cdot \mathbf{D}) \\ \text{Op}_D &= (\mathbf{M} : \epsilon) (\mathbf{v} \cdot \mathbf{D})\end{aligned}\quad (6)$$

and we keep in mind that $\mathbf{M} : \epsilon$ acts on the source coordinates (θ_s, ϕ_s) , $\mathbf{v} \cdot \mathbf{D}$ on the receiver coordinates (θ_r, ϕ_r) and the operator $(-\nabla_1^2)^i$ on the running coordinates on the sphere (θ, ϕ) . The addition theorem for spherical harmonics gives (Edmonds 1960):

$$\sum_m Y_l^{m*}(\theta_s, \phi_s) Y_l^m(\theta_r, \phi_r) = f Y_l^0(\Delta), \quad (7)$$

where Δ is the epicentral distance and f is the normalizing factor:

$$f = \sqrt{\frac{k}{2\pi}}, \text{ with } k = l + \frac{1}{2}.$$

Also:

$$\begin{aligned}\sum_m Y_l^{m*}(\theta_s, \phi_s) Y_l^m(\theta, \phi) &= f Y_l^0(\lambda) \\ \sum_m Y_l^{m*}(\theta, \phi) Y_l^m(\theta_r, \phi_r) &= f Y_l^0(\beta),\end{aligned}\quad (8)$$

where λ and β are angular distances SQ and RQ on the sphere, and Q is any point on the surface of the sphere, as defined in Fig. 4. Applying (7) and (8), we can now write:

$$\Lambda_K = \sum_{i=0}^{i=2} J_i,$$

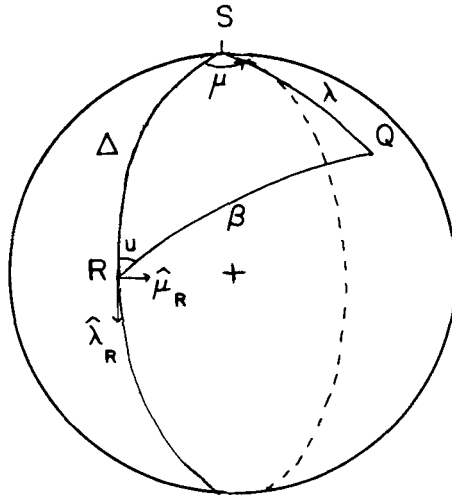


Figure 4. Epicentral coordinate system (λ, μ) used in the derivation of the first-order asymptotics. The great circle γ containing the source (S) and the receiver (R) defines the meridian of zero longitude. Q is any point on the sphere and $\hat{\lambda}_R, \hat{\mu}_R$ are unit vectors for the spherical coordinate system attached to point R .

where:

$$[2l(l+1)]^i J_i = \frac{\int \int \delta \omega_i^K(\theta, \phi) \mathbf{Op}_N^i[Y_l^0(\lambda) Y_l^0(\beta)] ds}{\mathbf{Op}_D[Y_l^0(\Delta)]} \quad (9)$$

In what follows, we shall derive an order $(1/l)$ asymptotic approximation to the location parameter, valid for any moment tensor source. We shall make use of the first-order asymptotic approximation to the fully normalized Legendre function X_l^m (Robin 1958):

$$X_l^m(x) = \frac{1}{\pi \sqrt{\sin x}} \cos \left[kx - \frac{\pi}{4} + m \frac{\pi}{2} + \left(\frac{m^2}{2k} - \frac{1}{8k} \right) \cot x \right] + O \left(\frac{1}{l^2} \right), \quad (10)$$

where X_l^m is related to Y_l^m by:

$$Y_l^m(\theta, \phi) = X_l^m(\theta) \exp(im\phi).$$

From here on, we shall work in an epicentral coordinate system (λ, μ) , with the epicentre S at the pole, and the great circle γ as the meridian of longitude zero (Fig. 4). We shall first consider the case of an isotropic source, already studied by Dahlen (1982, unpublished) and reported in Davis & Henson (1986). We shall be using a different approach, using a method based on the stationary phase approximation, and then extend the calculations to the case of a general moment tensor source observed on all three components.

In all cases considered, we can show by the method proposed below, that both J_1 and J_2 are of order $(1/l^2)$, so that we shall only be concerned with the calculation of J_0 (equation 9).

2 Case of an isotropic source observed on the vertical component

In this simple case, we obtain:

$$Y_l^0(\Delta) J_0 = \int \int \delta \omega_0^K(\lambda, \mu) Y_l^0(\lambda) Y_l^0(\beta) ds \quad (11)$$

and we clearly see from (11) and Fig. 4 how the contribution of each scattering point Q on the sphere contributes. Let us first set:

$$I(\lambda) = \int_0^{2\pi} \delta \omega_0^K(\lambda, \mu) Y_l^0(\beta) d\mu. \quad (12)$$

Using the asymptotic expression (10), we can write:

$$I(\lambda) = \int_0^{2\pi} g(\lambda, \mu) \cos \left(k\beta - \frac{\pi}{4} - \frac{\cot \beta}{8k} \right) d\mu$$

with:

$$g(\lambda, \mu) = \frac{\delta \omega_0^K(\lambda, \mu)}{\pi \sqrt{\sin \beta}}.$$

The contribution I_0 to $I(\lambda)$ (to order $1/l$) from the neighbourhood of the stationary point $\mu = 0$ can readily be obtained, using the results of Appendix A, and noting that, with the

notations of that appendix:

$$g_0 = \frac{\omega_0}{\pi \sqrt{\sin \beta_0}} \quad \text{with } \omega_0 = \delta \omega_0^K(\lambda, 0)$$

$$g_2 = \omega_2 - \frac{\cot \beta_0}{2} \beta_0'' \omega_0 \quad \text{with } \omega_2 = \frac{\partial^2 \delta \omega_0^K}{\partial \mu^2}(\lambda, 0),$$

where:

$$\beta_0 = \beta(\lambda, 0) \quad \text{and} \quad \beta_0'' = \frac{\partial^2 \beta}{\partial \mu^2}(\lambda, 0).$$

Then, to order $1/l$:

$$I_0 \simeq \frac{1}{\pi} \sqrt{\frac{2\pi}{k \sin \lambda \sin \Delta}} \left[\cos(k\beta_0) \omega_0 - \frac{\sin k\beta_0}{k} \left(\frac{\omega_2}{2\beta_0''} + \frac{\omega_0}{8\beta_0''} \right) \right] + O\left(\frac{1}{l^2}\right). \quad (13)$$

It can be shown, by the same procedures, that the contribution I_π from the stationary point $\mu = \pi$ to $I(\lambda)$ is such that:

$$Y_l^0(\Delta) J_0 = \int_0^\pi [I_0(\lambda) + I_\pi(\lambda)] Y_l^0(\lambda) \sin \lambda d\lambda = \int_0^{2\pi} I_0(\lambda) Y_l^0(\lambda) \sin \lambda d\lambda, \quad (14)$$

where $Y_l^0(\lambda)$ is replaced by its asymptotic expression (10).

Relation (14) corresponds to the fact that the contributions from $\mu = 0$ and $\mu = \pi$ add up to span the entire great circle γ (Fig. 4). This will be true in all cases studied in this paper, so that, in what follows, we shall only be concerned with calculating contributions I_0 from the stationary point $\mu = 0$.

Using (10), (13) and (14), we then obtain, to order $1/l$:

$$Y_l^0(\Delta) J_0 = \frac{1}{\pi \sqrt{\sin \Delta}} \left[\Omega_0 \cos \left(k\Delta - \frac{\pi}{4} \right) + \frac{\Omega_2}{2k} \sin \left(k\Delta - \frac{\pi}{4} \right) \right. \\ \left. + \frac{\Omega_0}{8k} \cot \Delta \sin \left(k\Delta - \frac{\pi}{4} \right) \right] + O\left(\frac{1}{l^2}\right), \quad (15)$$

where we have defined:

$$\Omega_0 = \frac{1}{2\pi} \int_0^{2\pi} \delta \omega_0^K(\lambda, 0) d\lambda$$

$$\Omega_2 = \frac{1}{2\pi} \int_0^{2\pi} \frac{\partial^2 \delta \omega_0^K}{\partial \mu^2}(\lambda, 0) (\cot \Delta - \cot \lambda) d\lambda. \quad (16)$$

Since we can show by the same method, that the integrals J_1 and J_2 are of order $1/l^2$, we then have:

$$\Lambda_K = J_0 + O\left(\frac{1}{l^2}\right).$$

Using the asymptotic expression (10) for $Y_l^0(\Delta)$, the terms in $\cot \Delta$ in (15) and (10) cancel

out and we finally obtain:

$$\Lambda_K = \Omega_0 + \frac{\Omega_2}{2k} \tan \left(k\Delta - \frac{\pi}{4} \right) + O \left(\frac{1}{l^2} \right). \quad (17)$$

As shown in Appendix B, this expression is equivalent to that of Dahlen in Davis & Henson (1986).

We note that, by using the classical stationary phase approximation to order zero and the corresponding asymptotic expression for X_l^m , we would have obtained again, in a straightforward manner using relations on the sphere, the zeroth-order geometrical optics approximation $\Lambda_k \simeq \Omega_0$ derived by Jordan (1978) and Dahlen (1979) using different approaches.

3 Case of a source represented by a moment tensor (M_{ij})

3.1 VERTICAL COMPONENT (SPHEROIDAL MODES)

In this case:

$$\mathbf{v} \cdot \mathbf{D} Y_l^0(\beta) = y_1(a) Y_l^0(\beta) = Y_l^0(\beta), \quad (18)$$

where a is the Earth's radius and y_1 is the displacement eigenfunction, in the notation of Alterman, Jarosch & Pekeris (1959) and Saito (1967), normalized to 1 at the surface, and:

$$\mathbf{M} : \epsilon Y_l^0(\lambda) = a_0 X_l^0(\lambda) + a_1(\Phi) X_l^1(\lambda) + a_2(\Phi) X_l^2(\lambda) \quad (19)$$

where, following the notations of Kanamori & Cipar (1974) and introducing the moment tensor $\{M_{ij}\}$ (Aki & Richards (1980):

$$fa_0 = \frac{1}{2} M_{rr} K_0$$

$$fa_1(\Phi) = K_1 \sqrt{l(l+1)} (+M_{r\theta} \cos \Phi + M_{r\phi} \sin \Phi) \quad (20)$$

$$fa_2(\Phi) = K_2 l(l+1) [(M_{\theta\theta} - M_{\phi\phi}) \cos 2\Phi + 2M_{\theta\phi} \sin 2\Phi] / 2,$$

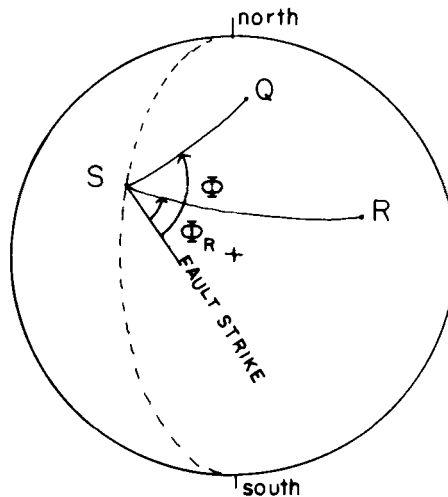


Figure 5. Definition of the azimuth angles Φ and Φ_R , measured from the strike of the fault.

where $\Phi = \Phi_R + \mu$ and the angle Φ_R , measured from the strike of the fault, is defined in Fig. 5. K_0 , K_1 and K_2 are linear combinations of eigenfunctions as defined in Kanamori & Cipar (1974) and calculated at the depth of the source.

In the first of equations (20), we have assumed that the trace of the moment tensor is zero, an assumption not critical to the validity of the present calculations.

We can rearrange $a_1(\Phi)$ and $a_2(\Phi)$, so that:

$$\begin{aligned} a_1(\Phi) &= A_1 \cos \mu + B_1 \sin \mu \\ a_2(\Phi) &= A_2 \cos 2\mu + B_2 \sin 2\mu \end{aligned} \quad (21)$$

with:

$$A_1 = a_1(\Phi_R)$$

$$A_2 = a_2(\Phi_R)$$

$$B_1 = \partial_\phi A_1 = \frac{K_1 \sqrt{l(l+1)}}{f} [-M_{r\theta} \sin \Phi_R + M_{r\phi} \cos \Phi_R] \quad (22)$$

$$B_2 = \frac{1}{2} \partial_\phi A_2 = \frac{K_2 l(l+1)}{f} [-(M_{\theta\theta} - M_{\phi\phi}) \sin 2\Phi_R + 2M_{\theta\phi} \cos 2\Phi_R]$$

This yields:

$$\text{Op}_D[Y_l^0(\Delta)] J_0 = a_0 S_0 + A_1 S_1 + A_2 S_2 + B_1 T_1 + B_2 T_2, \quad (23)$$

where:

$$\begin{aligned} S_0 &= \int \int \delta\omega_0^K(\lambda, \mu) Y_l^0(\lambda) Y_l^0(\beta) ds \\ S_1 &= \int \int \delta\omega_0^K(\lambda, \mu) X_l^1(\lambda) X_l^0(\beta) \cos \mu ds \\ S_2 &= \int \int \delta\omega_0^K(\lambda, \mu) X_l^2(\lambda) X_l^0(\beta) \cos 2\mu ds \\ T_1 &= \int \int \delta\omega_0^K(\lambda, \mu) X_l^1(\lambda) X_l^0(\beta) \sin \mu ds \\ T_2 &= \int \int \delta\omega_0^K(\lambda, \mu) X_l^2(\lambda) X_l^0(\beta) \sin 2\mu ds. \end{aligned} \quad (24)$$

Each of the integrals (24) can be evaluated using the stationary phase approximation to order $1/l$ of Appendix A and the asymptotic expressions (10). We obtain in this manner:

$$\begin{aligned} \text{Op}_D[Y_l^0(\Delta)] J_0 &= \Omega_0 [(a_0 - A_2) Q_1 - A_1 R_1] + \frac{\Omega_2}{2k} [(a_0 - A_2) R_1 + A_1 Q_1] \\ &+ \Omega_0 \cot \Delta \left[\frac{R_1(\Delta)}{8k} a_0 + \left(\frac{1}{8k} - \frac{1}{2k} \right) Q_1(\Delta) A_1 + \left(\frac{2}{k} - \frac{1}{8k} \right) R_1(\Delta) A_2 \right] \\ &+ B_1 \frac{Q_1(\Delta) \Omega_1}{k} - 2B_2 \frac{R_1(\Delta) \Omega_1}{k}, \end{aligned} \quad (25)$$

where we have defined:

$$Q_1(\Delta) = \frac{1}{\pi\sqrt{\sin \Delta}} \cos \left(k\Delta - \frac{\pi}{4} \right)$$

$$R_1(\Delta) = \frac{1}{\pi\sqrt{\sin \Delta}} \sin \left(k\Delta - \frac{\pi}{4} \right) \quad (26)$$

and introduced:

$$\Omega_1 = \frac{1}{2\pi} \int_0^{2\pi} \frac{\partial \delta \omega_0^K}{\partial \mu} (\lambda, 0) (\cot \Delta - \cot \lambda) d\lambda. \quad (27)$$

For the demoninator, we have:

$$\text{Op}_D[Y_l^0(\Delta)] = a_0 X_l^0(\Delta) + A_1 X_l^1(\Delta) + A_2 X_l^2(\Delta). \quad (28)$$

Replacing here also the Legendre functions by their asymptotic expressions (10), the terms in $\cot \Delta$ of (25) and (28) cancel out and we finally obtain:

$$\Lambda_K \simeq \Omega_0 + \frac{1}{2k} \Omega_2 \left(\frac{T+t}{1-tT} \right) + \frac{\Omega_1}{k} \left[\frac{B_1 - 2B_2 T}{(a_0 - A_2)(1-tT)} \right], \quad (29)$$

where:

$$T = \tan \left(k\Delta - \frac{\pi}{4} \right)$$

$$t = \frac{A_1}{a_0 - A_2}.$$

Equation (29) can also be written:

$$\Lambda_k \simeq \Omega_0 + \left(\frac{\Omega_2}{2k} + x \frac{\Omega_1}{k} \right) \tan \left(k\Delta - \frac{\pi}{4} + z \right) + y \frac{\Omega_1}{k} \quad (30)$$

with:

$$x = \frac{B_1 A_1 - 2B_2 (a_0 - A_2)}{A_1^2 + (a_0 - A_2)^2}$$

$$y = \frac{B_1 (a_0 - A_2) + 2B_2 A_1}{A_1^2 + (a_0 - A_2)^2} \quad (31)$$

and $\tan z = t$.

Again, this result is equivalent to that reported in Davis & Henson (1986), as shown in Appendix B. We note here that y/l is of order $1/l^2$.

3.2 HORIZONTAL COMPONENTS

To order $(1/l)$, we expect some contribution of spheroidal motion to the transverse component and toroidal motion to the longitudinal component.

Indeed, for spheroidal modes, the contribution to the longitudinal component comes from the term:

$$\mathbf{v} \cdot \mathbf{D}[Y_l^0(\beta)] = \hat{\lambda}_R y_3(a) \nabla_1[Y_l^0(\beta)] = y_3(a) \frac{\partial Y_l^0}{\partial \beta}(\beta) \cos(\pi - u), \quad (32)$$

where u is defined in Fig. 4 and, in the spherical triangle SRQ , we have the relation:

$$\frac{\sin u}{\sin \lambda} = \frac{\sin \mu}{\sin \beta} \quad (33)$$

y_3 is the displacement eigenfunction in the notation of Saito (1967).

In the same manner, the contribution to the transverse component comes from:

$$\mathbf{v} \cdot \mathbf{D}[Y_l^0(\beta)] = \hat{\mu}_R y_3(a) \nabla_1[Y_l^0(\beta)] = y_3(a) \frac{\partial Y_l^0}{\partial \beta}(\beta) \sin(\pi - u). \quad (34)$$

Similar relations can be obtained for toroidal modes.

3.2.1 Spheroidal modes: contribution to the longitudinal component

Just as in the case of the vertical component, we have here:

$$\mathbf{M} : \epsilon[Y_l^0(\lambda)] = a_0 X_l^0(\lambda) + a_1(\Phi) X_l^1(\lambda) + a_2(\Phi) X_l^2(\lambda).$$

Again, we can write:

$$\mathbf{Op}_D[Y_l^0(\Delta)] J_0 = a_0 S_0^L + A_1 S_1^L + A_2 S_2^L + B_1 T_1^L + B_2 T_2^L \quad (36)$$

with, now using (32):

$$\begin{aligned} S_0^L &= \int \int \delta \omega_0^K(\lambda, \mu) X_l^0(\lambda) \frac{\partial Y_l^0}{\partial \beta}(\beta) (-\cos u) ds \\ S_1^L &= \int \int \delta \omega_0^K(\lambda, \mu) X_l^1(\lambda) \frac{\partial Y_l^0}{\partial \beta}(\beta) (-\cos u) \cos \mu ds \end{aligned} \quad (37)$$

etc.

These integrals can be readily evaluated by the same method as used previously, using, in addition, the following asymptotic approximation, valid to order $(1/l)$ and obtained from (10) using the recurrence relation (B5) of Appendix B:

$$\frac{\partial Y_l^m}{\partial \beta}(\beta) = \frac{\sqrt{l(l+1)}}{\pi \sqrt{\sin \beta}} \left[\cos \left(k\beta - \frac{\pi}{4} + m \frac{\pi}{2} + \frac{\pi}{2} - \left[\frac{1}{8k} - \frac{(m^2+1)}{2l} \right] \cot \beta \right) \right] \quad (38)$$

We thus obtain:

$$\begin{aligned} \mathbf{Op}_D(Y_l^0(\Delta)) J_0 &= -\Omega_0 [(a_0 - A_2) R_1 + A_1 Q_1] + \frac{\Omega_2}{2k} [(a_0 - A_2) Q_1 - A_1 R] \\ &+ \Omega_2 \cot \Delta \left[-a_0 Q_1 \left(\frac{1}{2k} - \frac{1}{8k} \right) + \left(\frac{1}{k} - \frac{1}{8k} \right) R_1 A_1 \right. \\ &\left. + \left(\frac{5}{2k} - \frac{1}{8k} \right) Q_1 A_2 \right] + \frac{\Omega_1}{k} (B_1 R_1 + 2B_2 Q_1). \end{aligned} \quad (39)$$

For the denominator, we now have:

$$\mathbf{Op}_D[Y_1^0(\Delta)] = a_0 \frac{\partial Y_l^0}{\partial \Delta}(\Delta) + A_1 \frac{\partial Y_l^1}{\partial \Delta}(\Delta) + A_2 \frac{\partial Y_l^2}{\partial \Delta}(\Delta). \quad (40)$$

Using (38), (39) and (40), the terms in $\cot \Delta$ cancel out and we obtain:

$$\begin{aligned} \Lambda_K^{SL} &= \Omega_0 - \frac{\Omega_2}{2k} \left[\frac{(a_0 - A_2) Q_1 - A_1 R_1}{(a_0 - A_2) R_1 - A_1 Q_1} \right] + \frac{\Omega_1}{k} \left[\frac{B_1 R_1 + 2B_2 Q_1}{(a_0 - A_2) R_1 + A_1 Q_1} \right] \\ &= \Omega_0 + \tan \left(k\Delta - \frac{\pi}{4} + z + \frac{\pi}{2} \right) \left(\frac{\Omega_2}{2k} + x \frac{\Omega_1}{k} \right) + O \left(\frac{1}{l^2} \right), \end{aligned} \quad (41)$$

where x, y, z are as defined in (31).

We note that there is a $\pi/2$ shift in the phase of the fluctuations of Λ_K with angular order l , as compared to the vertical component, the amplitudes remaining equal.

3.2.2 Spheroidal modes: contribution to the transverse component

Using (34), (35), (40) and the order $(1/l)$ stationary phase approximation, we obtain:

$$\Lambda_K^{ST} = \frac{1}{k \sin \Delta} (\alpha \Omega_3 + \beta \Omega_0) \tan \left(k\Delta - \frac{\pi}{4} + z + \frac{\pi}{2} \right) + O \left(\frac{1}{l^2} \right) \quad (41)$$

with:

$$\begin{aligned} \alpha &= \frac{(a_0 - A_2) A_2}{(a_0 - A_2)^2 + A_1^2} - 1 \\ \beta &= \frac{-B_1 A_1 + 2B_2(a_0 - A_2)}{(a_0 - A_2)^2 + A_1^2} \end{aligned} \quad (43)$$

and we have defined:

$$\Omega_3 = \frac{1}{2\pi} \int_0^{2\pi} \frac{\partial \delta \omega_0^K}{\partial \mu}(\lambda, 0) d\lambda. \quad (44)$$

3.2.3 Toroidal modes: contribution to the transverse component

In what follows, we shall call K a given toroidal mode, not to be confused with the spheroidal mode previously considered. In this case:

$$\mathbf{M} : \epsilon Y_l^0(\lambda) = c_1(\Phi) X_l^1(\lambda) + c_2(\Phi) X_l^2(\lambda) \quad (45)$$

with, using the notation of Kanamori & Cipar (1974):

$$\begin{aligned} c_1(\Phi) &= -L_1 q_L = -L_1(M_{r\phi} \cos \Phi - M_{r\theta} \sin \Phi) = C_1 \cos \mu + D_1 \sin \mu \\ c_2(\Phi) &= L_2 p_L = L_2 \left[M_{\theta\phi} \cos 2\Phi - \frac{1}{2}(M_{\theta\theta} - M_{\phi\phi}) \sin 2\Phi \right] \\ &= C_2 \cos 2\mu + D_2 \sin 2\mu, \end{aligned} \quad (46)$$

where L_1 and L_2 are eigenfunctions calculated at the depth of the source and

$$C_1 = c_1(\Phi_R)$$

$$C_2 = c_2(\Phi_R)$$

$$D_1 = \partial_\phi C_1 = L_1(M_{r\phi} \sin \Phi_R + M_{r\theta} \cos \Phi_R)$$

$$D_2 = \frac{1}{2} \partial_\phi C_2 = L_2 \left[-M_{\theta\phi} \sin 2\Phi_R - \frac{1}{2}(M_{\theta\theta} - M_{\phi\phi}) \cos 2\Phi_R \right]. \quad (47)$$

In this case:

$$\mathbf{Op}_D[Y_l^0(\Delta)]J_0 = \int \int \delta\omega_0(\lambda, \mu) [c_1 X_l^1(\lambda) + c_2 X_l^2(\lambda)] \frac{\partial Y_l^0}{\partial \beta}(\beta) (-\cos u) ds \quad (48)$$

and:

$$\mathbf{Op}_D[Y_l^0(\Delta)] = C_1 \frac{\partial X_l^1}{\partial \Delta} + C_2 \frac{\partial X_l^2}{\partial \Delta}. \quad (49)$$

This yields, using (10) and (38) and the stationary phase approximation of Appendix A:

$$\Lambda_K^{TT} = \Omega_0 + \left(\frac{\Omega_2}{2k} + \frac{\Omega_1}{k} x_T \right) \tan \left(k\Delta - \frac{\pi}{4} + z_T \right) + O \left(\frac{1}{l^2} \right), \quad (50)$$

where Ω_0 is the great circle average of the local frequency corresponding to toroidal mode K , and:

$$\begin{aligned} \tan z_T &= \frac{D_1}{C_1} \\ x_T &= \frac{2D_2C_2 + D_1C_1}{C_1^2 + C_2^2}. \end{aligned} \quad (51)$$

3.2.4 Toroidal modes: contribution to the longitudinal component

Following the same procedure, we obtain:

$$\Lambda_K^{TL} = \frac{1}{k \sin \Delta} (\alpha^T \Omega_3 + \beta^T \Omega_0) \tan \left(k\Delta - \frac{\pi}{4} + z_T \right) + O \left(\frac{1}{l^2} \right) \quad (52)$$

with z_T defined in (51) and:

$$\begin{aligned} \alpha^T &= \frac{C_1^2 + 2C_2^2}{C_1^2 + C_2^2} \\ \beta^T &= \frac{2D_2C_2 + D_1C_1}{C_1^2 + C_2^2}. \end{aligned} \quad (53)$$

From equation (52), we see that there is an order $(1/l)$ contribution of toroidal modes to the longitudinal component. We therefore do not expect to obtain identical results on the vertical and longitudinal component when measuring spheroidal mode eigenfrequencies, unless we can eliminate the higher order effects.

4 Synthetic experiments

We have just seen that the horizontal components contain to order $1/l$, contributions from both spheroidal and toroidal modes whereas the vertical component only has contributions from spheroidal motion, expressed rather simply in equation (30). In what follows, we shall only consider the simplest case of the vertical component. We shall also assume that we have been able, for instance by variable filtering, to isolate a given mode K . The examples will be given for the case of the fundamental spheroidal mode. We will focus our attention on angular orders greater than 20, not only because the asymptotics are valid at large angular orders, but also because, in the $l = 10$ –20 range, effects of coupling with the rotation of the Earth are likely to disturb the pattern of fluctuations (Masters, Park & Gilbert 1983).

The first-order asymptotics give the following expression for the location parameter corresponding to spheroidal mode K and measured on the vertical component:

$$\Lambda_K = A(l) + \frac{B(l)}{l} \tan \left(k\Delta - \frac{\pi}{4} + z \right) \quad (54)$$

with:

$$A(l) = \Omega_0$$

$$B(l) = \frac{\Omega_2}{2} + x \Omega_1$$

and x, z depend on the source parameters and have been defined in (31).

The fluctuations of the eigenfrequency as a function of angular order l have a periodicity which is governed by the epicentral distance Δ , which enters the argument of the term in tangent. Such a periodicity is clearly observed, as we have seen in Fig. 1. Two other parameters are essential to the actual appearance of the data: the zero crossings and sense of the fluctuations (up or down after zero crossing) in other words, their phase, governed by the value z , that is, by the source parameters (equations 30, 31), and by the epicentral distance. The other parameter is the amplitude of the fluctuations, which depends on the factor $B(l)$ in front of the tangent, that is on the structure in the neighbourhood of the great circle.

In what follows, we shall consider some experiments designed to gain insight into the sensitivity of the observations to each of the parameters involved.

4.1 MEASUREMENT ERRORS

We first would like to give some indication of the significance of the signal level in the fluctuations which we observe. The real observational error is difficult to estimate in such a study, since we are not able to repeat measurements for different earthquakes with the same source-station geometry. Following Dahlen (1976), we have estimated the error due to noise in the data, by calculating the spectrum of the noise in the time period preceding the earthquakes considered. In the frequency range of interest ($l = 20$ –70), our calculations show that the noise contribution to the relative deviation in eigenperiod is no greater than 1×10^{-3} , typically of the order of 0.5×10^{-3} .

For the particular problem studied here, this procedure is however not totally satisfying, since, in our measurements, we are including small peaks, whose shape rarely resembles that of a perfect resonance function. In particular, we expect some systematic errors to occur, not related to the lateral heterogeneity, but having the same fluctuating behaviour as a function of angular order, and which could be due to mode overlap (Xu Guoming, Knopoff

& Zürn 1983). To investigate this further, we have calculated synthetic seismograms for fundamental mode Rayleigh waves in a spherically symmetric earth model (PREM) for different source-station geometries and source mechanisms, corresponding to the data analysed in this paper. Then the synthetic seismograms were put through the same processing as we do for the real data. This includes tapering of the time series with a Connes window function $w(x) = 16x^2(1-x)^2$ and time variable filtering (Roullet & Romanowicz 1984). We used different lengths of time series (12, 24, 36 hr) and measured eigenfrequencies with the same method as for real data (peak frequencies). The resulting relative departures of eigenperiods with respect to the PREM model are shown in Fig. 6 for the Costa Rica event of 1983 April 3, observed at SSB ($\Delta = 82.2^\circ$), and in Fig. 7 for the same event observed at PAF ($\Delta = 133.8^\circ$). In these figures, calculations were made without including noise in the data. It is clear that systematic fluctuations are present, and have the same periodicity as in the real data, but when the length of record is increased, their

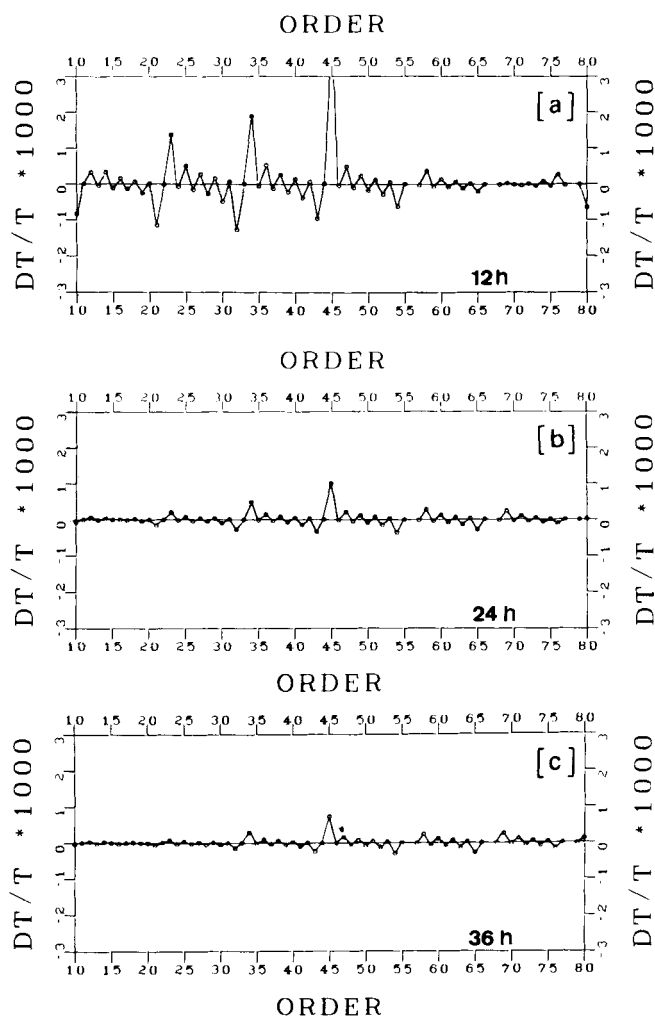


Figure 6. Synthetic calculations of relative eigenperiod shifts with respect to PREM for a noise-free seismogram corresponding to the case of the Costa Rica event of 1983 March 4 observed at station SSB, for three different lengths of record, starting at the origin time: (a) 12 hr, (b) 24 hr, (c) 36 hr ($\Delta = 82^\circ$).

amplitude decreases considerably. For a typical record length of 24 hr, as used in this paper, and except for the smallest peaks ($l = 34$ and 45 in Fig. 6, $l = 18, 49, 57$ in Fig. 7), the systematic relative error is found not to exceed in general 0.1×10^{-3} , which is well below the level of observed fluctuations (Figs 16 and 17).

In the presence of pre-existing noise in the data (as well as noise from overtones), the amplitude of errors is not dramatically increased, but the systematic fluctuation pattern in the synthetics is somewhat destroyed. When Earth noise is present, there is a trade-off for the optimal length of record to take in order to minimize errors, since, the signal to noise ratio deteriorates after some time.

The results of these experiments show that, provided care is taken to choose the length of record appropriately, the observed fluctuations are not dominated by noise and do contain some information about higher order effects of lateral heterogeneity.

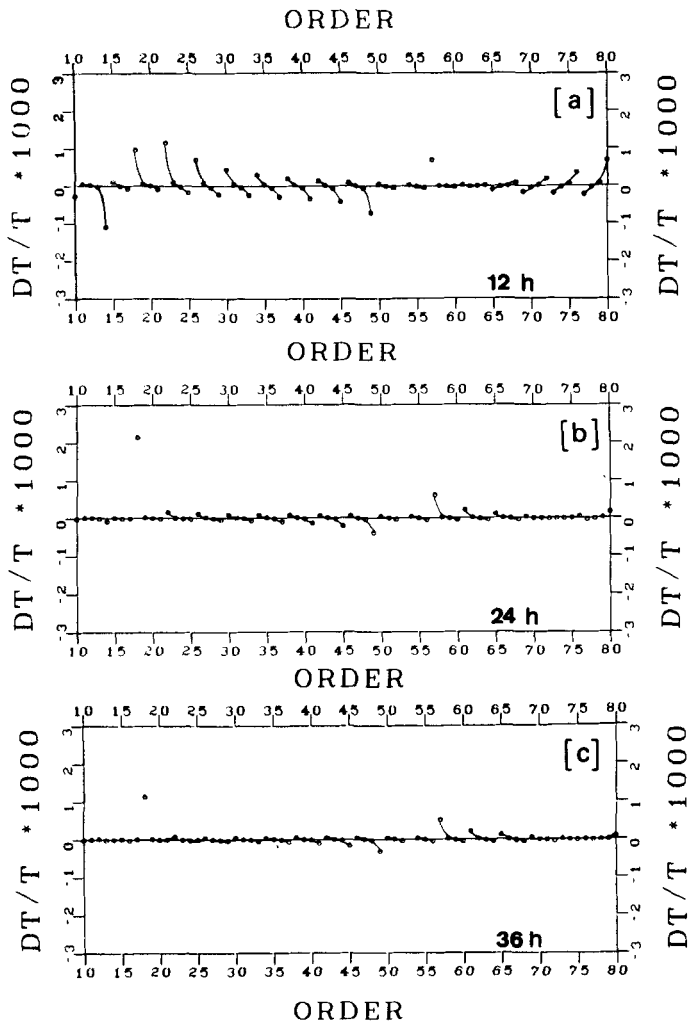


Figure 7. Same as Fig. 6, for the Costa Rica event observed at station PAF ($\Delta = 133.76^\circ$).

4.2 SOURCE MECHANISM

In Fig. 8, we compare observed fluctuations as a function of angular order l , for the Costa Rica event of 1983 April 3, observed at the GEOSCOPE station SSB, with synthetic calculations using two different solutions for the source, both given in the PDE bulletins: one is the centroid solution obtained by the CMT method of Dziewonski, Chou & Woodhouse (1981), the other is the P -wave inversion of USGS. Variable filtering has been applied to the data to isolate the fundamental mode. The smooth part, in the observations, has been removed by high pass filtering. In the synthetics, only the first-order term in A/l

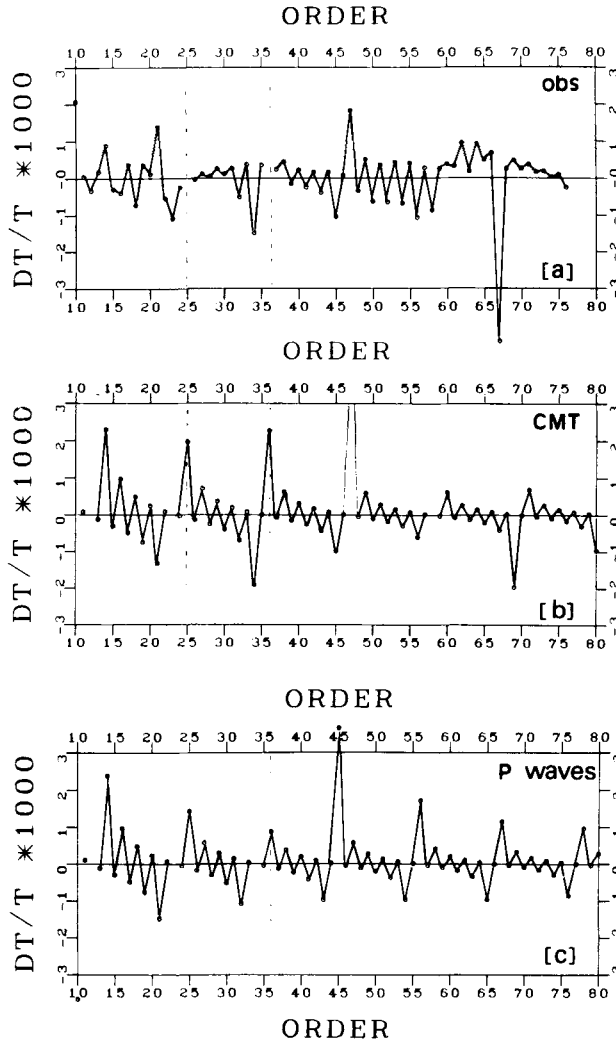


Figure 8. Costa Rica event of 1983 April 3, observed at GEOSCOPE station SSB (vertical component): comparison of observed fluctuations as a function of angular order (a) with synthetics, for two different source solutions, (b) CMT centroid solution ($\phi = 108^\circ$, $\delta = 67^\circ$, $\lambda = 81^\circ$, $h = 28$ km) and (c) P -wave moment tensor inversion ($\phi = 125^\circ$, $\delta = 75^\circ$, $\lambda = 90^\circ$, $h = 37$ km). The epicentral distance is fixed at $\Delta = 82.55^\circ$ corresponding to the CMT epicenter. Notations are as in Fig. 1 and the smooth part of the observations has been removed by high pass filtering. The reference model is PREM. See text for additional description.

$\tan X$ has been considered, the factor A being taken as constant and adjusted to match the order of magnitude of the observed amplitudes. The epicentral distance is fixed here at $\Delta = 82.55^\circ$. In this example, we shall only discuss the phase of the fluctuations.

In this case, we see that the observations (8a) present consecutive positive maxima for angular order of $l = 25, 36$ and 47 , with associated minima for $l = 23, 34$ and 45 . This behaviour is well matched by the synthetic in (8b), corresponding to the CMT centroid solution. The P -wave solution, however, matches the first two maxima, but the third one is shifted to $l = 45$. We are thus tempted to conclude that the centroid solution matches the data better, which is not surprising since it is obtained with somewhat longer period data, more comparable to the period range of the present observations. We see that a relatively

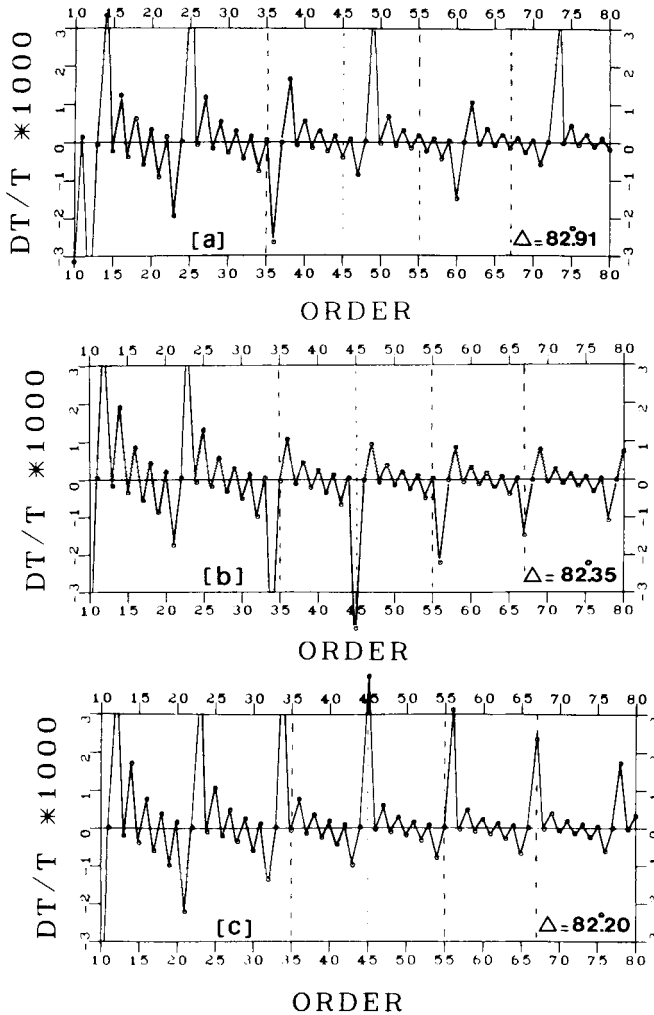


Figure 9. Comparison of three synthetic calculations for the Costa Rica event of 1983 April 3, with varying epicentral distance. (a) $\Delta = 82.91^\circ$, (b) $\Delta = 82.35^\circ$, (c) $\Delta = 82.20^\circ$. The source parameters are fixed at the CMT solution and only the term in tangent is considered, with a constant multiplicative factor, the same in all cases.

small change in the source mechanism (17° in strike, 8° in dip and slip, and depth 9 km) can introduce a significant shift in the phase of the fluctuations. We note that the match of the CMT solution is not perfect over the whole period range considered (between $l = 65$ and 70), which can be an effect of the source but also could be due to the epicentral distance chosen, as will be seen below.

4.3 EPICENTRAL DISTANCE

Fig. 9 is a comparison of the results of three synthetic calculations, again for the Costa Rica event of 1983 March 4, observed on the vertical component at SSB. The source mechanism

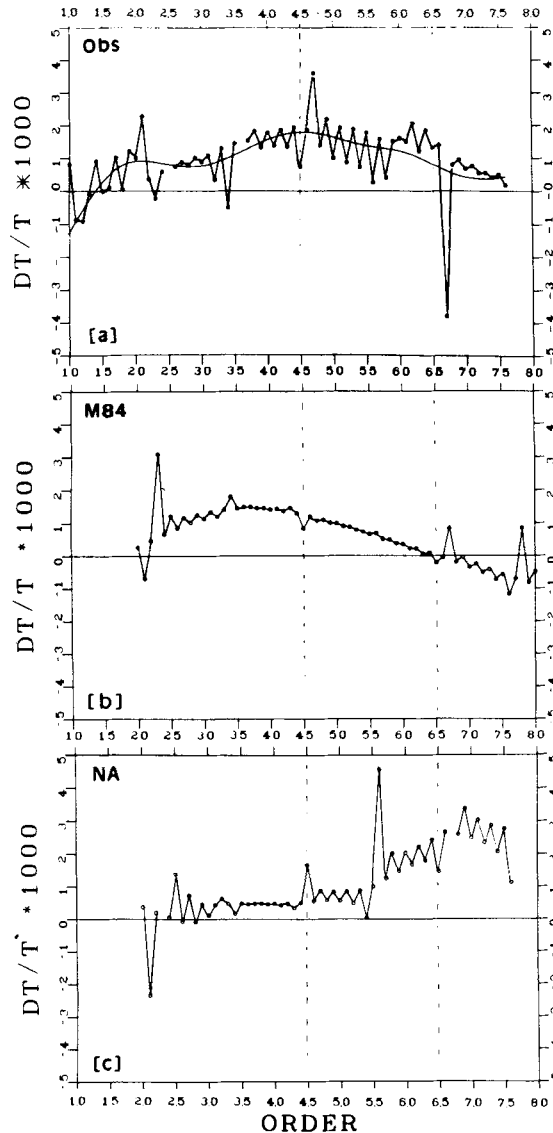


Figure 10. Costa Rica event observed at SSB (vertical component): comparison of observations (a) with synthetics obtained using two different laterally heterogeneous earth models; (b) M84 of Woodhouse & Dziewonski (1984); (c) NA of Nakanishi & Anderson (1984). Notation is as in Fig. 1 but the smooth part of the observations has not been removed. The source parameters and epicentral distance are fixed and correspond to the CMT solution.

is now fixed at the CMT solution, and the epicentral distance is varied. We see that, as we increase Δ , the phase of the fluctuations changes rapidly. This is particularly visible in the case of extrema (when $\tan X$ goes to infinity) around orders $l = 35, 45$ and 55 . The best match with the observations (Fig. 8a) is obtained for $\Delta \cong 82.4^\circ$, as will be seen in Section 5. The sensitivity to epicentral distance leads us, as will be seen in that section, to introduce a search for the best fitting Δ .

4.4 EARTH STRUCTURE

As noted above (see Section (54)), the amplitude of the fluctuations with l depends on the Earth's structure in the neighbourhood of the great circle, through the terms Ω_1 and Ω_2 and so does the smooth part of the spectrum, which depends on the great circle average Ω_0 .

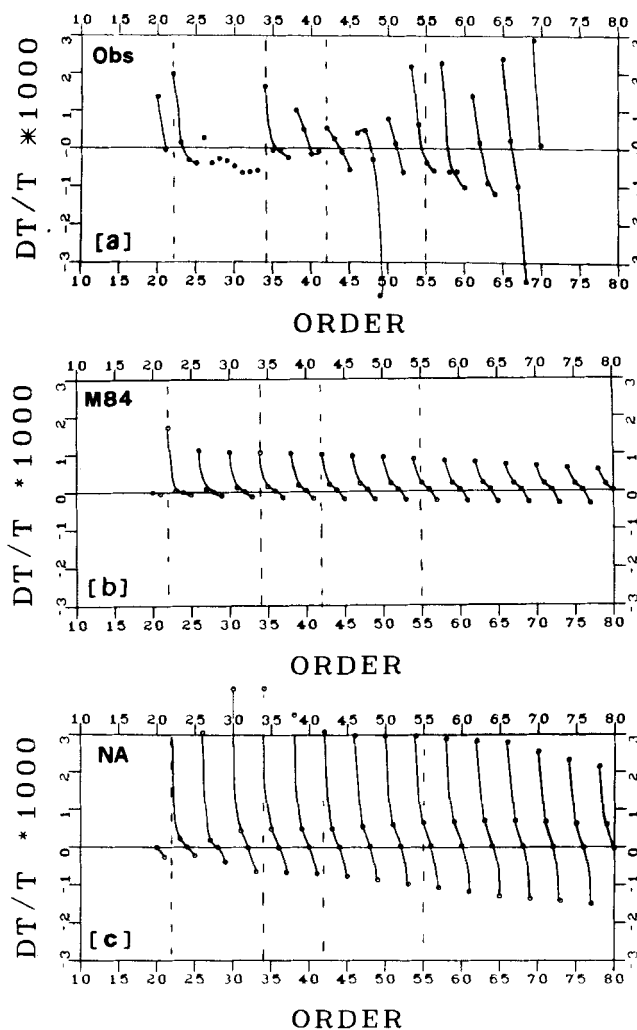


Figure 11. Same as Fig. 10 for the Costa Rica event of 1983 April 4 observed at GEOSCOPE station PAF with the smooth part removed both from observations (a) and from synthetics (b), model M84, (c) model NA.

Figs 10, 11 and 12 show examples of comparisons of observations with synthetics, using two available long-period global models, M84 of Woodhouse & Dziewonski (1984) and a model we call NA (Nakanishi & Anderson 1984). For both models, we have used the spherical harmonic expansion over the Earth of the local frequency $\delta\omega_0$ which these papers provide, and calculated Ω_0 , Ω_1 and Ω_2 from it. In both examples, the source mechanism, depth and epicentral distance are fixed as given for the CMT solution in the PDEs. The relative deviations of eigenperiods are calculated with respect to the PREM model (Dziewonski & Anderson 1981).

Fig. 10 corresponds to the Costa Rica event observed at SSB, where, this time, we have not removed the smooth part of the observations. It is interesting to note that neither model matches the data satisfactorily. The smooth part of the spectrum, in this example, is overall better matched by M84 than by NA, but the amplitude of the fluctuations is too small for M84.

In Fig. 11, we give a second example, for the Costa Rica event of 1983 April 4, observed

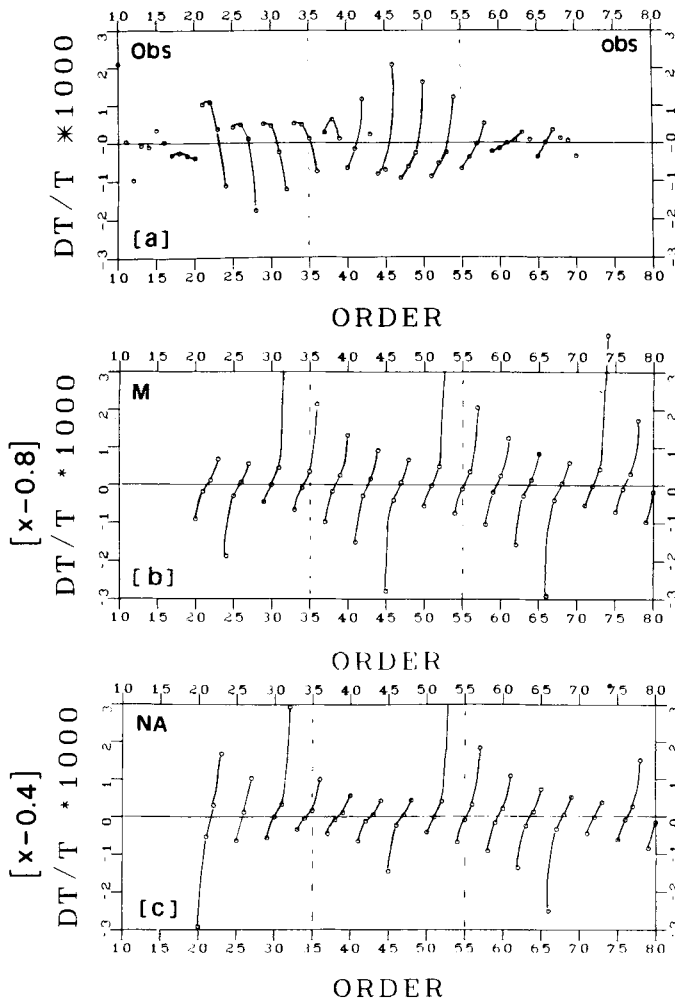


Figure 12. Same as Fig. 11 for the Chagos event of 1983, November 30, observed at GEOSCOPE station PAF. Smooth part also removed ($\Delta = 42.95^\circ$, $h = 10$ km).

at PAF. Here, we have removed the smooth part from the observations by high pass filtering and only considered the order $(1/l)$ tangent term in the synthetics as well. Again model NA matches the amplitudes of the observed fluctuations better than M84 above $l = 45$.

In Fig. 12, we give a third example, for the Chagos event of 1983 November 30, observed at GEOSCOPE station PAF (Kerguelen). Here again we have removed the smooth part from the observations by high pass filtering and we note the characteristic order 4 periodicity in the fluctuations, corresponding to an epicentral distance close to 45° . In the synthetics, we only show the first-order term in $\tan X$. The synthetic data have been multiplied by -0.8 , in the case of model M84, and -0.4 in the case of NA, to match the order of magnitude and sense of variations of the observed fluctuations in the order range $l = 35-55$. This particular example shows greater complexity, part of which may be due to the source (there are clear shifts in the phase): none of the models succeeds in matching the π shift in phase of the trend of the fluctuations around $l = 35$.

These three examples (and there are many more, see e.g. Davis & Henson 1986) show that the global large-scale models available at present are still somewhat inadequate to explain data on particular great circle paths. More importantly to us here, there is clearly some additional information contained in the amplitudes of the fluctuations, that could be exploited to constrain global earth models better.

5 First attempts at inversion

Equation (54) shows that, when the source parameters and epicentral distance are fixed, the relation between the observed eigenfrequency, as a function of l , and the Earth functionals $A(l)$ and $B(l)$ is linear. It is therefore straightforward to set up an inversion procedure to determine A and B . This is our present goal, and we show here some preliminary results based on two examples: the Costa Rica event of 1983 April 3, observed at SSB and PAF.

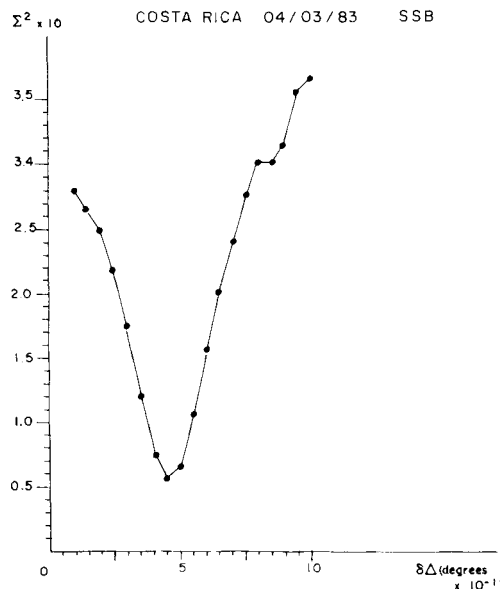


Figure 13. Residuals versus Δ (epicentral distance) curve for the inversion of vertical component observations of the Costa Rica event of 1983 April 3 at station SSB. The zero in the abscissae corresponds to $\Delta = 81.96^\circ$.

In order to model the variation with l of coefficients A and B , we have divided the range in l considered into several intervals and, in each of these, expressed A and B as linear combinations of cubic splines, defined so as to keep smooth transitions from one interval to the next. Let N be the total number of splines χ_i used ($n = 4$ times the number of intervals). We then have:

$$A(l) = \sum_{i=1}^N a_i \chi_i(l)$$

$$B(l) = \sum_{i=1}^N b_i \chi_i(l)$$

and we set up the inverse problem as:

$$\Omega_{\text{obs}} - \Omega_{\text{ref}}(l) = \sum_{i=1}^N \left\{ a_i + \frac{b_i}{l} \tan X(l) \right\} \chi_i(l) \quad (55)$$

and solve for a_i and b_i (a total of $2N$ coefficients) by least squares, assuming $X(l)$ is known.

We can vary the size and length of the intervals to investigate the stability of the solution and put weights on individual data points, since removing the largest extrema often helps improve the overall fit.

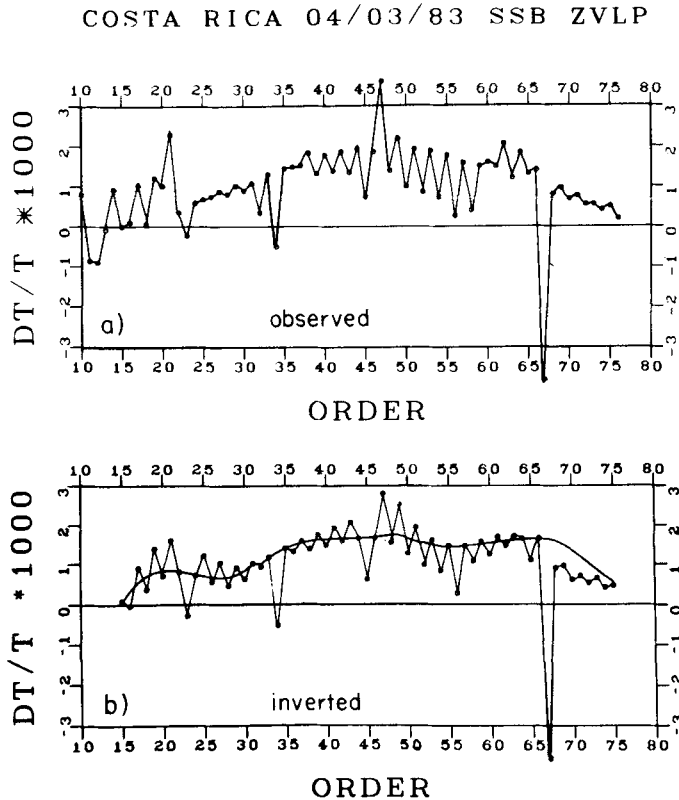


Figure 14. Comparison of (a) observed eigenfrequencies as a function of angular order to (b) computed ones after inversion, for the Costa Rica event of 1983 April 3, on the vertical component at SSB. The solid line in (b) is the great circle average Ω_0 as obtained by inversion.

In this experiment, the source parameters are kept fixed at the CMT solution of Fig. 8. This constraint can later be removed and the search for best fitting mechanism, which acts on the phase of the fluctuations, introduced into the inversion procedure. As seen earlier, the influence of the epicentral distance can be strong and we can search for the best fitting value of Δ and determine Δ_0 for which the least squares residual after inversion is minimized. Fig. 13 gives an example of the residuals versus Δ curve obtained for the case of observations at station SSB. The minimum at $\Delta = 82.41^\circ \pm 0.03^\circ$ is clearly resolvable.

In Fig. 14 we compare the observed eigenfrequencies (a) with the calculated ones (b), after inversion. The solid line in Fig. 12(b) is the great circle average Ω_0 , as calculated by inversion, and we see that we can match the observed fluctuations rather well. In fact, in both this example and the next, we can explain 95 per cent of the variance in the data. The length of each interval for the definition of the spline polynomials is here 16 (in units of l). Fig. 15 shows similar results for the case of the Costa Rica event observed at station PAF, with a length of 14 for the intervals defining the splines.

6 Extension to amplitude data

So far, we have only considered observations pertaining to the eigenfrequencies of normal modes of the Earth, putting aside any amplitude data. However, observations of similar fluctuations on measurements of the quality factor Q are also available. One such example, for the great Sumba earthquake of 1977 August 19, was given in Roult *et al.* (1986). In Fig.

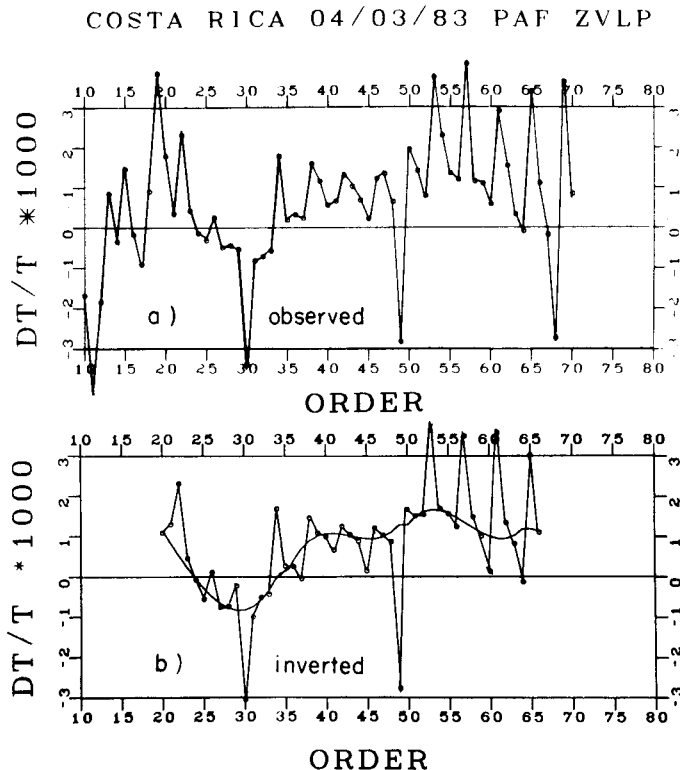


Figure 15. Same as Fig. 14 for the Costa Rica event of 1983 April 3, observed on the vertical component at station PAF.

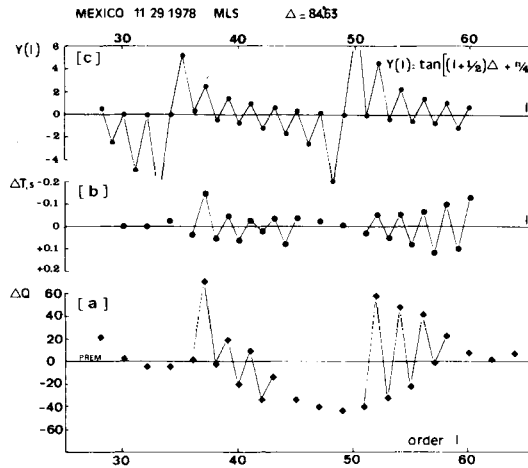


Figure 16. Quality factor (a) and eigenperiods (b) as a function of angular order for the Mexican event of 1978 November 29, observed on the vertical component at IPG station MLS (Moulis, France), after variable filtering to isolate the fundamental mode. The data are expressed as departures from the PREM model. At the top, (c), the variation of $\tan [(l + 1/2) \Delta - \pi/4]$ is given for comparison.

16, we give another example, for the Mexico event of 1978 November 29, observed on the vertical component at IPG station MLS (Moulis, Pyrenees), corresponding to an epicentral distance close to 90° . We show here observations of both eigenperiods (smooth part removed) and quality factor, expressed as departures from the PREM model and compared to the theoretical term $\tan (k\Delta - \pi/4)$, neglecting the additional angle z due to the source mechanism. The Q measurements have been obtained by a method described in Roullet (1975), using the decay of amplitudes with time, and variable filtering has first been applied to the data in order to isolate the fundamental mode.

The fact that such fluctuations should be observed in the amplitudes is not in itself surprising, in view of the theoretical expressions obtained from first order perturbation theory (Woodhouse 1984). If we neglect terms due to coupling between modes, the amplitude of mode K is indeed given by:

$$A_K = \sum_m R_m^K S_m^K \left(l - \frac{2\Lambda_K}{\omega_K} \right), \quad (56)$$

where R_m^K and S_m^K have been defined in Section 2 and ω_K is the eigenfrequency of mode K calculated for the reference spherically symmetric model (here Λ_K is calculated with a slightly different definition of the splitting matrix). This implies that the attenuation factor will contain, through $2\Lambda_K/\omega_K$, a term in $\tan (k\Delta - \pi/4)$.

In the case of amplitudes, however, we cannot set up an inverse problem at present, since terms coming from the coupling between modes are likely to contribute to the first-order asymptotics. This will be the subject of a later communication.

7 Conclusions

We have shown that a significant amount of coherent information is contained in the fluctuations with angular order of observed eigenfrequencies, adding to the variance in the data. By using first-order asymptotics, it is possible to retrieve: (1) more accurate

estimates of the great circle average Ω_0 of the local frequency, and (2) estimates of the derivatives of Ω_0 , which will yield additional constraints on the structure in the neighbourhood of each great circle. First attempts at inversion of single station, single mode eigenfrequency data, using as wide a frequency band as possible, look promising. The analysis by such a method of a collection of single station measurements over a set of great circles covering the Earth should provide better constraints on the even part of lateral heterogeneity in the Earth's mantle and increase significantly the amount of data variance that can be explained.

Acknowledgments

The contents of this paper have greatly benefited from stimulating discussions with R. Madariaga and N. Jobert. The short unpublished note of Dahlen (1982) has inspired us to investigate the intricacies of higher order asymptotics. We also thank P. Davis and I. Henson for sending us a preprint of their paper, and H. Kanamori for making available to us a tape with model M84. Discussions with W. Zürn and E. Wielandt have helped us gain insight into the problem of systematic errors. This work was conducted with the help of INSU grant ATP 11-33. IPG contribution no. 898.

References

- Aki, K. & Richards, P., 1980. *Quantitative Seismology*, W. H. Freeman, San Francisco.
- Alterman, Z., Jarosch, H. & Pekeris, C. L., 1959. Oscillations of the Earth, *Proc. R. Soc., Ser. A*, **252**, 80-95.
- Backus, G., 1964. Geographical interpretation of measurements of average phase velocities of surface waves over great circle and great semi circular paths, *Bull. seism. Soc. Am.*, **54**, 571-610.
- Burridge, R., 1962. The reflexion of high frequency sound in a liquid sphere, *Proc. R. Soc., Ser. A*, **270**, 144-153.
- Dahlen, F. A., 1976. Models of the lateral heterogeneity of the Earth consistent with eigenfrequency splitting data, *Geophys. J. R. astr. Soc.*, **44**, 77-105.
- Dahlen, F. A., 1979. The spectra of unresolved split normal mode multiplets, *Geophys. J. R. astr. Soc.*, **58**, 1-34.
- Davis, P. & Henson, I., 1986. Validity of the great circular average approximations for inversion of normal mode measurements, *Geophys. J. R. astr. Soc.*, in press.
- Dziewonski, A. & Anderson, D. L., 1981. Preliminary Reference Earth Model, *Phys. Earth planet. Int.*, **25**, 297-456.
- Dziewonski, A. M., Chou, T.-A. & Woodhouse, J. H., 1981. Determination of earthquake source parameters from waveform data for studies of global and regional seismicity, *J. geophys. Res.*, **86**, 2825-2852.
- Edmonds, A. R., 1960. *Angular Momentum in Quantum Mechanics*, Princeton University Press, New Jersey.
- Gradshteyn, I. S. & Ryzhik, I. M., 1965, *Tables of Integrals, Series and Products*, Academic Press, London.
- Jobert, N. & Roullet, G., 1976. Periods and damping of free oscillations observed in France after 16 earthquakes, *Geophys. J. R. astr. Soc.*, **45**, 155-176.
- Jordan, T. H., 1978. A procedure for estimating lateral variations from low frequency eigenspectra data, *Geophys. J. R. astr. Soc.*, **52**, 441-455.
- Kanamori, H. & Cipar, J., 1974. Focal process of the great Chilean earthquake of May 22, 1960, *Phys. Earth planet. Int.*, **9**, 128-136.
- Masters, G., Park, J. & Gilbert, F., 1983. Observations of coupled spheroidal and toroidal modes, *J. geophys. Res.*, **88**, 10 285-10 298.
- Nakanishi, I. & Anderson, D. L., 1984. Measurements of mantle wave velocities and inversion for lateral heterogeneity and anisotropy - II. Analysis by the single-station method, *Geophys. J. R. astr. Soc.*, **78**, 573-617.

- Robin, L., 1958. *Fonctions sphériques de Legendre et fonctions sphéroïdales*, Gauthiers Villars, Paris.
- Romanowicz, B., Cara, M., Fels, J. F. & Roullet, D., 1984. GEOSCOPE: a French initiative in long period three component global seismic networks, *Eos, Trans. Am. geophys. Un.*, **65**, 753–756.
- Roullet, G., 1975. Attenuation of seismic waves of very low frequency, *Phys. Earth planet. Int.*, **10**, 159–166.
- Roullet, G. & Romanowicz, B., 1984. Very long period data from the GEOSCOPE network: preliminary results on great circle averages of fundamental and higher Rayleigh and Love modes, *Bull. seism. Soc. Am.*, **74**, 2221–2243.
- Roullet, G., Romanowicz, B. & Jobert, N., 1986. Observations of departures from classical approximations on very long period GEOSCOPE records, *Annls. Geophys.*, in press.
- Saito, M., 1967. Excitation of free oscillations and surface waves by a point source in a vertically heterogeneous Earth, *J. geophys. Res.*, **72**, 3689–3699.
- Silver, P. & Jordan, T. H., 1981. Fundamental spheroidal mode observations of aspherical heterogeneity, *Geophys. J. R. astr. Soc.*, **64**, 605–634.
- Woodhouse, J. H., 1984. The joint inversion of seismic waveforms for lateral variations in Earth structure and earthquake source parameters, in *Earthquakes: Observation, Theory and Interpretation*, eds Kanamori, H. & Boschi, E., *Proc. Int. School Phys. Enrico Fermi*, **85**, 366–397.
- Woodhouse, J. & Dahlen, F. A., 1978. The effect of a general aspherical perturbation on the free oscillations of the earth, *Geophys. J. R. astr. Soc.*, **53**, 335–354.
- Woodhouse, J. H. & Dziewonski, A. M., 1984. Mapping the upper mantle: three dimensional modelling of earth structure by inversion of seismic waveforms, *J. geophys. Res.*, **89**, 5953–5986.
- Woodhouse, J. H. & Girnius, T. P., 1982. Surface waves and free oscillations in a regionalized earth model, *Geophys. J. R. astr. Soc.*, **68**, 653–673.
- Worzel, J. L., Ewing, M. & Pekeris, C. L., 1948. Propagation of sound in the ocean, *Mem. geol. Soc. Am.*, **27**, part II.
- Xu Guoming, Knopoff, L. & Zürn, W., 1983. Variations of period and Q of free oscillations due to mode overlap, *Geophys. J. R. astr. Soc.*, **72**, 709–719.

Appendix A: approximation of integrals by the method of stationary phase to order $(1/l)$

Let $I(\lambda)$ be of the form:

$$I(\lambda) = \int_A^B g(\lambda, \mu) \cos[kF(\mu)] d\mu$$

where $k = l + 1/2$.

We know how to evaluate the contribution to this integral from the neighbourhood of a stationary point μ_0 , such that $F'(\mu_0) = 0$, using the approximation of stationary phase to order zero (e.g. Burridge 1962). If we want the approximation to be valid to order $(1/l)$, we need to expand g and F in the Taylor series around μ_0 , keeping as many terms as necessary:

$$g(\lambda, \mu) = g_0 + ug_1 + \frac{u^2}{2} g_2 + \dots$$

$$F(\mu) = F_0 + \frac{u^2}{2} F'' + \frac{u^3}{3!} F''' + \frac{u^4}{4!} F'''' + \dots$$

where we have set: $u = \mu - \mu_0$

$$g_0 = g(\lambda, \mu_0); \quad g_1 = \frac{\partial g}{\partial \mu}(\lambda, \mu_0); \quad g_2 = \frac{\partial^2 g}{\partial \mu^2}(\lambda, \mu_0);$$

$$F'' = \frac{\partial^2 F}{\partial \mu^2}(\mu_0); \quad F''' = \frac{\partial^3 F}{\partial \mu^3}(\mu_0); \quad F'''' = \frac{\partial^4 F}{\partial \mu^4}(\mu_0);$$

To evaluate the contribution I_0 to $I(\lambda)$ from the neighbourhood of μ_0 , we can extend the

limits of integration to infinity and write, to order $1/l$:

$$I_0 = \text{Re} (A + B + C)$$

where:

$$A = g_0 \exp (ikF_0) \int \exp (ik) \left(u^2 \frac{F''}{2} + u^3 \frac{F'''}{3!} + u^4 \frac{F''''}{4!} \right) d\mu$$

$$B = g_1 \exp (ikF_0) \int u \exp \left(ik \frac{u^2}{2} F'' \right) d\mu$$

$$C = \frac{g_2}{2} \exp (ikF_0) \int u^2 \exp \left(ik \frac{u^2}{2} F'' \right) d\mu.$$

Pekeris (Worzel, Ewing & Pekeris 1948) gives an expression for the term A :

$$A = \left[g_0 \exp \left[i \left(kF_0 \pm \frac{\pi}{4} \right) \right] \right] \sqrt{\frac{2\pi}{k|F''|}} \left[1 + \frac{ih}{k} + O \left(\frac{l}{k^2} \right) \right]$$

where the term in (ih/k) is added to the classical order zero stationary phase approximation, with:

$$h = \frac{5(F''')^2}{24(F'')^3} - \frac{1}{8} \frac{F''''}{(F'')^2}.$$

The \pm sign is $+$ if $F'' > 0$ and $-$ if $F'' < 0$.

Furthermore, we have $B = 0$, since

$$\int x \exp (ikx) dx = 0$$

and, in the calculation of C , we use the classical result:

$$\int x^2 \exp (i\alpha x^2) dx = \sqrt{\frac{\pi}{\alpha}} \exp \left(\pm i \frac{\pi}{4} \right) \frac{i}{2\alpha}$$

with $+$ if $\alpha > 0$, $-$ if $\alpha < 0$. Then:

$$C = \frac{g_2}{2} \exp \left[i \left(kF_0 \pm \frac{\pi}{4} \right) \right] \sqrt{\frac{2\pi}{k|F''|}} \left(\frac{i}{kF''} \right).$$

Finally:

$$I_0 = \sqrt{\frac{2\pi}{k|F''|}} \left[\cos \left(kF_0 \pm \frac{\pi}{4} \right) g_0 - \frac{1}{k} \sin \left(kF_0 \pm \frac{\pi}{4} \right) \left(hg_0 + \frac{g_2}{2F''} \right) + O \left(\frac{1}{l^2} \right) \right]. \quad (\text{A1})$$

Application to the calculation of the location parameter

In the present application, $F(\mu)$ is of the form:

$$kF(\mu) = k\beta - \frac{\pi}{4} + m \frac{\pi}{2} + \frac{n}{k} \cot \beta$$

where m and n are integers, and (Fig. 4):

$$\cos \beta = \cos \lambda \cos \Delta + \sin \lambda \sin \Delta \cos \mu,$$

β being chosen so that $0 < \beta < \pi$.

The stationary points of F are, to order $(1/l)$, those of β . We have:

$$\sin \beta \frac{\partial \beta}{\partial \mu} = \sin \lambda \sin \Delta \sin \mu.$$

The stationary points are therefore $\mu = 0$ and $\mu = \pi$. This corresponds, as expected, to points located on the great circle containing the source and the receiver (Fig. 4). We then have:

$$\frac{\partial^2 F}{\partial \mu^2}(0) = \frac{\partial^2 \beta}{\partial \mu^2}(0) = \frac{\sin \lambda \sin \Delta}{\sin \beta_0} = \beta_0'' \text{ with } \cos \beta_0 = \cos(\lambda - \Delta).$$

Also:

$$F'''(0) = 0,$$

which yields:

$$h(0) = \frac{1}{8} \left(\frac{1}{\beta_0''} + 3 \cot \beta_0 \right). \quad (\text{A2})$$

In the same manner:

$$h(\pi) = \frac{1}{8} \left(\frac{1}{\beta_\pi''} + 3 \cot \beta_\pi \right). \quad (\text{A3})$$

Appendix B: evaluation of integrals Ω_1 and Ω_2 (equations 16 and 27)

Let us consider the spherical harmonic expansion of the local frequency $\delta\omega_0$:

$$\delta\omega_0(\lambda, \mu) = \sum_{l,m} \omega_l^m Y_l^m(\lambda, \mu). \quad (\text{B1})$$

Then, according to Backus (1964):

$$\Omega_0(\Theta, \Phi) = \frac{1}{2\pi} \int_{\gamma} \delta\omega_0(s) ds = \sum_{l,m} P_l(0) \omega_l^m Y_l^m(\Theta, \Phi) \quad (\text{B2})$$

where (Θ, Φ) are the coordinates of the pole of the great circle γ and P_l is the Legendre polynomial of degree l .

In the epicentral coordinate system of Fig. 4, we have:

$$\Omega_2 = \cot \Delta I_1 - I_2$$

where:

$$\begin{aligned} I_1 &= \frac{1}{2\pi} \int_0^{2\pi} \frac{\partial^2 \delta\omega_0}{\partial \mu^2}(\lambda, 0) d\lambda \\ I_2 &= \frac{1}{2\pi} \int_0^{2\pi} \cot \lambda \frac{\partial^2 \delta\omega_0}{\partial \mu^2}(\lambda, 0) d\lambda \end{aligned} \quad (\text{B3})$$

Then, using (B1), Backus' relation and (B2):

$$I_1 = \Sigma (-m^2) P_l(0) \omega_l^m Y_l^m \left(\frac{\pi}{2}, \frac{\pi}{2} \right) = \frac{\partial^2 \Omega_0}{\partial \Phi^2} \quad (\text{B4})$$

Also:

$$I_2 = \frac{1}{2\pi} \Sigma (-m^2) \omega_l^m \int_0^{2\pi} \cot \lambda Y_l^m(\lambda, 0) d\lambda$$

We can make use of the following recurrence relation (Gradshteyn & Ryzhik 1965):

$$\frac{\partial P_l^m}{\partial \lambda} = P_l^{m+1} + m \cot \lambda P_l^m \quad (\text{B5})$$

where P_l^m are Legendre functions (not normalized).

Let us set $X_l^m = a_l^m P_l^m$. Then:

$$I_2 = \sum_{l,m} m^2 \omega_l^m P_l(0) Y_l^{m+1} \left(\frac{\pi}{2}, \frac{\pi}{2} \right) \frac{a_l^m}{a_l^{m+1}}$$

and, using (B5) at $\lambda = \pi/2$:

$$I_2 = \Sigma (im) \omega_l^m P_l(0) \frac{\partial X_l^m}{\partial \Phi^2} \left(\frac{\pi}{2} \right) \exp(im\Phi) = \frac{\partial^2 \Omega_0}{\partial \Theta \partial \Phi} . \quad (\text{B6})$$

Hence:

$$\Omega_2 = \cot \Delta \frac{\partial^2 \Omega_0}{\partial \Phi^2} - \frac{\partial^2 \Omega_0}{\partial \Theta \partial \Phi} . \quad (\text{B7})$$

In the same manner:

$$\begin{aligned} \Omega_1 &= \frac{1}{2\pi} \cot \Delta \int_0^{2\pi} \frac{\partial \delta \omega_0}{\partial \mu}(\lambda, 0) d\lambda - \frac{1}{2\pi} \int_0^{2\pi} \cot \lambda \frac{\partial \omega_0}{\partial \mu}(\lambda, 0) d\lambda \\ &= \Sigma \omega_l^m P_l(0) \left\{ \cot \Delta im Y_l^m \left[\frac{\pi}{2}, \frac{\pi}{2} \right] + i \frac{\partial X_l^m}{\partial \Theta} \exp [i(m+1)\frac{\pi}{2}] \right\} \end{aligned}$$

or:

$$\Omega_1 = \cot \Delta \frac{\partial \Omega_0}{\partial \Phi} - \frac{\partial \Omega_0}{\partial \Theta} . \quad (\text{B8})$$

Expressions (B7) and (B8) are the same as those reported in the appendix of Davis & Henson (1986).